ISSN: 1686-8420 (Print), 2651-2289 (Online)

RMUTT Research Journal
Science and Technology
Rajamangala University of Technology Thanyaburi

Simulation of Shielding Parameters of Some High Entropy Alloys Containing Energies for Gamma Ray and Fast Neutron

Kittisak Sriwongsa[1,2*], Punsak Glumglomchit[3], Teeratus Wananuraksakul[3], Arisa Pimprakhon[3], Taweewat Hanchana[3] and Sunantasak Ravangvong[4]

[1]Lecturers responsible for Bachelor of Education Program in Physics, Faculty of Education, Silpakorn University, Nakhon Pathom, 73000, THAILAND

[2]The demonstration school of Silpakorn University, Nakhon Pathom, 73000, THAILAND Thailand

[3]Huahin Vitthayalai School, Hua–Hin, Prachuap Khiri Khan, 77110, THAILAND

[4]Division of Science and Technology, Faculty of Science and Technology, Phetchaburi Rajabhat University, Phetchaburi, 76000, THAILAND

[*]Corresponding author e-mail: Sriwongsa_k@silpakorn.edu

ARTICLE INFO

Article history:
Received: 24 April, 2020
Revised: 29 May, 2020
Accepted: 19 June, 2020
Available online: 23 June, 2020
DOI: 10.14456/rj-rmutt.2020.9

Keywords: alloy, mass attenuation coefficient, fast neutron

ABSTRACT

This work explains the theoretically radiation shielding of alloy materials by using WinXCom software program at energies ranging 1 keV-100 GeV and the density of alloy was computed by rule of mixture (ROM). The radiation shielding properties of some high entropy alloys (HEAs) were found dependent on energies ranging. At low energies ranging, the mass attenuation coefficient presented many intermittent shifts in accordance with the photoelectric effect absorption edges. At intermediate energies ranging, the mass attenuation coefficient value is nearly constant, and the effective atomic number was nearly the mean atomic number as the Compton scattering is main process. At high energies ranging, the pair production is main process and tends to be constant at high energies ranging. The effective atomic number and the electron density of alloy had the opposite tend. The mean free path and the half value layer had the same behavior. Among the selected alloys, the alloy only in composite Co-Cr-Fe-Ni was found to possess superior radiation shielding effectiveness due to its higher values of

ISSN: 1686-8420 (Print), 2651-2289 (Online)

both the mass attenuation coefficient and the effective atomic number and lower values of the electron density, the mean free path and the half value layer. In addition, the fast neutron removal cross-section was evaluated and discussed. It is found that the fast neutron removal cross–section values for the studied alloys in composite Co-Cr-Fe-Ni had highest value. The computation was useful for the potential application of alloys containing energies in the field of gamma-ray and neutron shielding medium.

INTRODUCTION

Since starting to study and design on high entropy alloys (HEAs), the indexed study output in Web of Science (WoS) indicates that high entropy alloys (HEAs) are an emerging layer of alloys that are lately being popularly studied (1-4). The alloy materials are found in many fields such as irradiation, nuclear reactors, engineering materials, petrochemical industries and biomedical implants (5-8). In the field of radiation physics and dosimetry, there are many important photon interaction parameters such as mass attenuation coefficient (μ_m), effective atomic number (Z_{eff}) and electron density (N_{el}) which helping in determine and design for radiation protection efficiency of medium (9,10).

Mass attenuation coefficient (μ_m) is common property of medium which studies the probability of interaction for gamma radiations with a medium. An effective atomic number (Z_{eff}) is property of mixture or compound like an atomic number of elements. So anyway, these values are feature based on energy, helps to display the efficacy for shielding of medium and interprets gamma radiations attenuation by a medium. Electron density (N_{el}) value is another common property of the medium, which lets data about the average number of electrons per unit mass of medium. Moreover, the partial density method is popularly use to research the fast neutron removal cross–section of shielding medium (11-13).

In this context, mass attenuation coefficients, effective atomic number, effective electron density, mean free path, half-value layer and fast neutron removal cross-section for alloys have been computed. The computation will give useful data for the alloy that was used in shielding medium applications.

MATERIALS AND METHODS

Density, ρ_{mix}, of alloys is the basic parameter using determined the important parameters which determined by the rule of mixture (ROM) by Eq. (1) (14):

$$\rho_{mix} = \frac{\sum_{i=1}^{n} c_i A_i}{\frac{\sum_{i=1}^{n} c_i A_i}{\rho_i}} \quad (1)$$

here ρ_i, c_i, and A_i are density, atomic fraction and atomic weight of element i^{th}, respectively.

The theoretical/method basis have been separated into the following sub-sections:

Radiation shielding parameters

The theoretical simulation of mass attenuation coefficients (μ_m) of alloy using WinXCom software program for a photon at energies range 1 keV-100 GeV by Eq. (2) (15,16):

$$\mu_m = \sum_i w_i (\mu_m)_i \quad (2)$$

here w_i and $(\mu_m)_i$ means mass fraction and mass attenuation coefficient of element i, respectively.

Effective atomic numbers (Z_{eff}) for alloy can be determined from Eq. (3) (15,16):

$$Z_{eff} = \frac{\sigma_{t,a}}{\sigma_{t,el}} \quad (3)$$

here $\sigma_{t,a}$ and $\sigma_{t,el}$ are total atomic and electronic cross-section, respectively and both values of cross-section are determined from Eq. (4) and (5) (15-17):

$$\sigma_{t,a} = \frac{\mu_m M}{N_A \sum_i n_i} \quad (4)$$

$$\sigma_{e,el} = \frac{1}{N_A} \sum_i \frac{f_i}{Z_i} A_i (\mu_m)_i \quad (5)$$

here M, n_i, N_A, f_i, Z_i and A_i are the molecular weight of mixture component in the alloy, oxygen atom number per each composition, Avogadro's number, respectively. μ_m and $(\mu_m)_i$ are mass attenuation coefficients and mass attenuation coefficient of element i, respectively.

Electron densities (N_{el}) for alloy refer to electrons number per unit mass were computed by formula Eq. (6) (16,17):

$$N_{el} = \frac{\mu_m}{\sigma_{t,el}} \quad (6)$$

Mean free path, MFP, is the average distance between two successive interactions of photons in medium and computed by following in Eq. (7) (17, 18):

$$MFP = \frac{1}{\mu} \quad (7)$$

The half-value layer (HVL) is a quantity describing the thickness of attenuator that attenuation of photon density to half of the incident energy as the lower of HVL value is better shielding effectiveness and can be calculated using Eq. (8) (19, 20):

$$HVL = \frac{0.693}{\mu} \quad (8)$$

here μ is linear attenuation coefficient which computed by multiplying of density and mass attenuation coefficient of a compound.

Fast neutron removal cross-section

The probability of the interaction for neutron with the medium can be discussed on macroscopic effective removal cross-section (Σ_R) and can be calculated by following in Eq. (9) (21-23):

$$\sum_R = \sum_i w_i \left(\frac{\sum_R}{\rho} \right)_i \quad (9)$$

ISSN: 1686-8420 (Print), 2651-2289 (Online)

here $(\Sigma_R/\rho)_i$ (cm^2/g) and w_i are mass removal cross-section of i^{th} constituent and partial density (g/cm^3), respectively.

RESULTS AND DISCUSSIONS

Gamma rays shielding properties of alloys were discussed by calculation of mass attenuation coefficient (μ_m), effective atomic numbers (Z_{eff}), effective electron density (N_{el}), mean free path (MFP), half-value layer (HVL) and fast neutron removal cross-section. The chemical compositions (wt%) of elements and density of aluminium (Al), cobalt (Co), chromium (Cr), iron (Fe), nickel (Ni) and titanium (Ti) alloys system are presented in Table 1.

Table1 The chemical compositions in wt. fraction and density (g/cm^3) of the alloy (1)

Sample	Wt. fraction of elements						Density
	Al	Co	Cr	Fe	Ni	Ti	(g/cm^3)
A0	-	0.2551	0.2347	0.2551	0.2551	-	8.09
A1	0.0698	0.2326	0.2326	0.2326	0.2326	-	7.55
A2	0.1304	0.2174	0.2174	0.2174	0.2174	-	7.12
A3	0.1837	0.2041	0.2041	0.2041	0.2041	-	6.76
A4	0.1667	0.1852	0.1852	0.1852	0.1852	0.0926	6.48

Table 2 The photon energies (in $\times 10^{-3}$ MeV) of absorption edges for elements.

Element	Al	Ti	Cr	Fe	Co	Ni
Atomic number (Z)	13	22	24	26	27	28
K	1.56	4.97	5.99	7.11	7.71	8.33
L1						1.01

Mass attenuation coefficient (μ_m)

Figure 1 presents the relationship between μ_m of alloys and energy. As figure 1, μ_m decreased rapidly at 0.001-0.1 MeV which photoelectric effect is the main interaction process, and slowly at 0.1-10 MeV which Compton scattering process is dominated, whereas start increases slowly at 10-10^5MeV as pair production is the main interaction process. The discontinuities in μ_m values were appeared in low energy range because of L and K absorption edges of elements as presented in table 2. From Figure 1, the sample A0 has the highest μ_m. All in all, it indicated that A0 is the best material for shielding radiation.

ISSN: 1686-8420 (Print), 2651-2289 (Online)

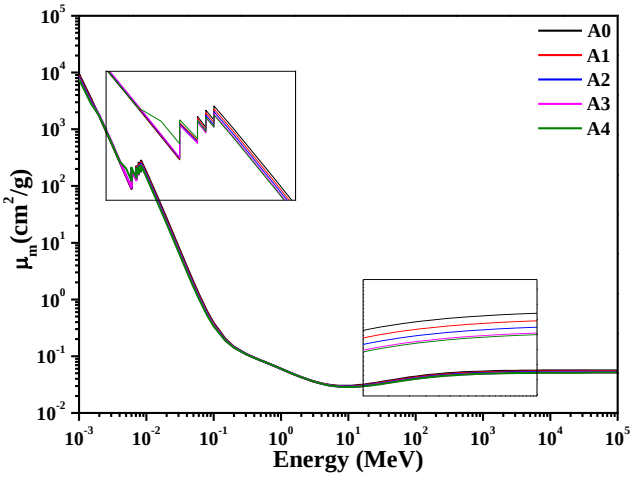

Figure 1 The μm of alloys with energy.

Effective atomic number (Z_{eff}) and electron density (N_{el})

Figure 2 presents the Z_{eff} of alloys at energies 10^{-3}-10^{5} MeV. In the limited energies range at 0.1 MeV-1.0 MeV, the Z_{eff} value of alloys decreased rapidly with increasing energy. During 1.0-150.0 MeV, the Z_{eff} value increased with increasing energy. The energies above 150 MeV, Z_{eff} value nearly constant was observed for all alloys. Z_{eff} value of alloy must stay in between the lowest atomic number (Z = 13) and highest atomic numbers (Z = 28) of ingredient elements (11). Among alloys, Z_{eff} maximum value was observed of A0 alloy in total energies range (having maximum content of Ni); whereas Z_{eff} minimum value was observed of A4 (having minimum content of Ni). Figure 3 presents the N_{el} of alloys with energy. It will be noted that the trend of N_{el} according to different energies is the same trend Z_{eff} value of alloy. So anyway, there are swing back in the trend i.e. A4 alloy shown N_{el} highest value whereas it had Z_{eff} lowest value. Similarly, A0 alloy had N_{el} lowest value whereas it shows the highest Z_{eff} value. The highest N_{el} value for A4 alloy can be attributed to the Ti content's alloy effect. The vacant sites in the structure of alloy were replaced by Ti atom which result in increased electron density of selected alloy medium.

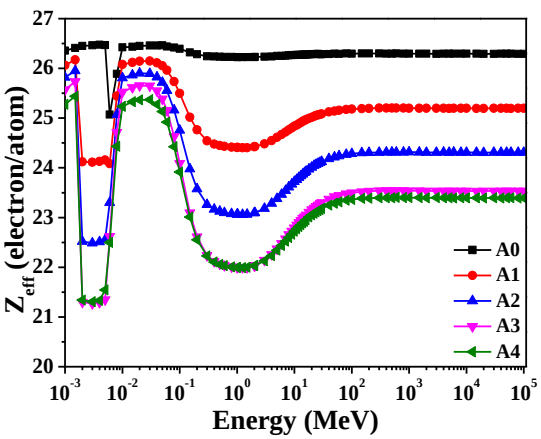

Figure 2 The Z_{eff} of alloys with energy.

ISSN: 1686-8420 (Print), 2651-2289 (Online)

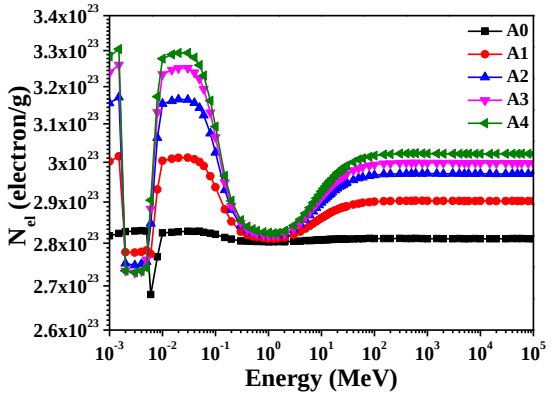

Figure 3 The N_{el} of alloys with energy.

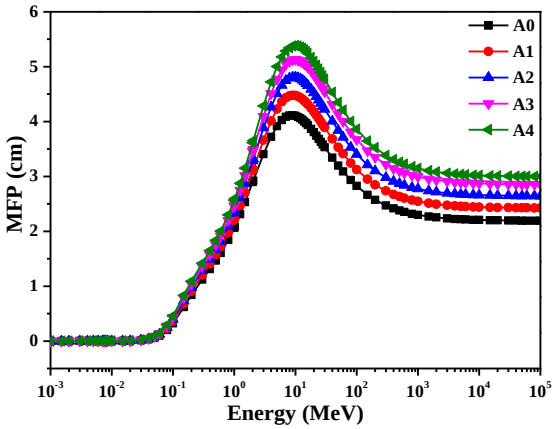

Figure 4 The MFP of alloys with energy.

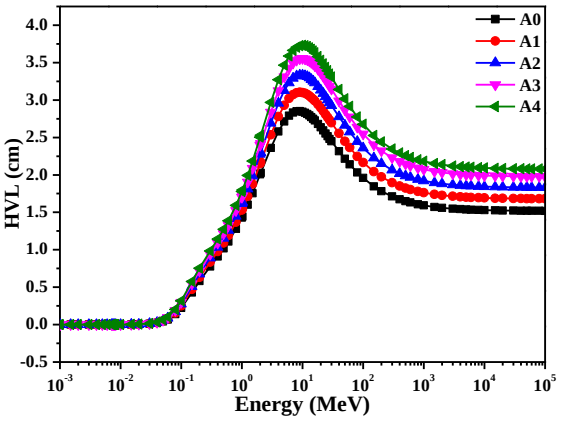

Figure 5 The HVL of alloys with energy.

Figures 4 and 5 show the MFP and HVL of the energy range at 1 keV-100 GeV. MFP and HVL values of alloys were increased with increasing photon energy. MFP and HVL value were seen very small from 1-100 keV and rise gradually with increasing energies until 8 MeV. After that, a slow rate of increase in MFP and HVL values with energies were registered at an energy ranging from 8 MeV-10 MeV. For energies > 10 MeV, MFP and HVL value shown exponential decreased with additional energies and becomes nearly constant at energies above 1000 MeV. This variation is acceptable in the light of reliance on cross–section value for different major photon interaction processes at different energies range.

The lower energies range, cross-section of the photoelectric absorption effect process was presented in inversely with energy as $E^{-3.5}$. It means, photon interaction probability at lower energy, photoelectric absorption effect will higher values and smaller thickness looks enough for absorption photons in investigated medium, on the other hand, increment in the thickness of interacting medium was required for photon interaction. Because of this high reliance on cross-section value on energy, MFP and HVL values swell gradually for chosen alloys. At intermediate energies range, the cross-section of the Compton scattering process is presented in linear relation with energies. Due to this weak dependence of cross-section value on energies, tends of MFP and HVL values increase with slow rates for chosen alloys. The cross–section of pair production process founds logarithmic with high energies range. So, with expansion at high energies, photon interaction of pair production probability tends to occur exponentially. Therefore, the thickness requirement may

ISSN: 1686-8420 (Print), 2651-2289 (Online)

decrease with a large amount of photon energies for better absorption in the medium.

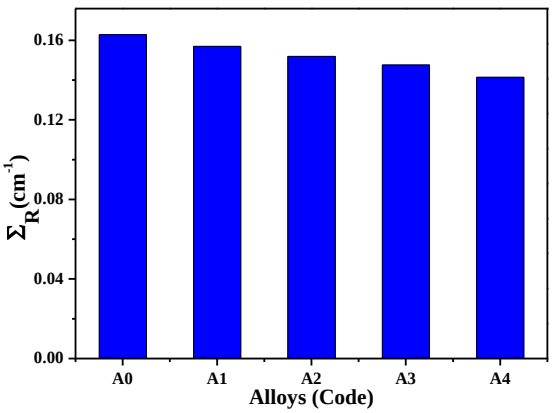

Figure 6 The Σ_R for alloys.

Fast neutron removal cross–section

The fast neutron removal cross–section Σ_R (cm^{-1}) value of alloys were exhibited in Figure 6. It found that Σ_R (cm^{-1}) of A0 was highest. Therefore, A0 alloy is the best neutron shielding compared with other alloys.

CONCLUSION

In summary, the value of mass attenuation coefficients, effective atomic numbers, effective electron densities, mean free path and half-value layer for alloys were determined by WinXCom software at energy range 1 keV–100 GeV. The result has shown that Z_{eff} and N_{el} values depend on the energies. The graph of interactions at low photon energy has peaks (absorption edges) because of the dominant photoelectric effect near L and K absorption edges of alloy composition. A0 alloy was found to have the lowest mean free path and half-value layer value. The results from this study indicated that A0 alloy is the best medium for gamma rays shielding applications. Also, the result of fast neutron removal cross–section value indicated that A0 is an excellent medium too.

ACKNOWLEDGEMENT

In this study, the authors would like to thank Phetchaburi Rajabhat University for its support instrument.

REFERRENCES

1. Qiu Y, Thomas S, Fabijanic D, Barlow AJ, Fraser HL, Birbilis N. Microstructural evolution, electrochemical and corrosion properties of $Al_xCoCrFeNiTi_y$ high entropy alloys. Mater Design. 2019;170:107698.
2. Alijani F, Reihanian M, Gheisari Kh. Study on phase formation in magnetic FeCoNiMnV high entropy alloy produced by mechanical alloying. J Alloy Compd. 2019;773:623-30.
3. Chen LB, Wei R, Tang K, Zhang J, Jiang F, Sun J. Ductile-brittle transition of carbon alloyed $Fe_{40}Mn_{40}Co_{10}Cr_{10}$ high entropy alloys. Mater Lett. 2019;236:416-19.
4. Jiang H, Jiang L, Qiao D, Lu Y, Wang T, Cao Z, et al. Effect of Niobium on Microstructure and Properties of the $CoCrFeNb_xNi$ High Entropy Alloys. J Mater Sci Technol. 2017;33:712-7.
5. Vishwanadh B, Vaibhav K, Jha SK, Mirji KV, Samajdar I, Srivastava D, et ai. Development of Nb-1%Zr-0.1%C alloy as structural components for high temperature reactors. J Nucl Mater. 2012;427:350-8.

ISSN: 1686-8420 (Print), 2651-2289 (Online)

6. Li X, Cheng Z, Hu K, Chen H, Yang C. Crystallization kinetics and spark plasma sintering of amorphous $Ni_{53}Nb_{20}Ti_{10}Zr_8Co_6Ta_3$ powders prepared by mechanical alloying. Vacuum. 2015;114:93-100.

7. Vishwanath PS, Badiger NM. Gamma ray and neutron shielding properties of some alloy materials. Ann Nucl Energy. 2014;64:301-10.

8. Jin W, Wu G, Li P, Paul KC. Improved corrosion resistance of Mg-Y-RE alloy coated with niobium nitride. Thin Solid Films. 2014;572:85-90.

9. Ruengsri S, Insiripong S, Sangwaranatee N, Kaewkhao J. Development of barium borosilicate glasses for radiation shielding materials using rice husk ash as a silica source. Prog Nucl Energ. 2015;83:99-104.

10. Mostafa AMA, Issa SAM, Sayyed MI. Gamma ray shielding properties of PbO-B_2O_3-P_2O_5 doped with WO_3. J Alloy Compd. 2017;708:294-300.

11. Singh H, Sharma J, Singh T. Extensive investigations of photon interaction properties for Zn_xTe_{100-x} alloys. Nucl Eng Technol. 2018;50:1364-71.

12. Kaur S, Singh KJ. Investigation of lead borate glasses doped with aluminium oxide as gamma ray shielding materials. Ann Nucl Energy. 2014;63:350-54.

13. Dong MG, Xue XX, Elmahroug Y, Sayyed MI, Zaid MHM. Investigation of shielding parameters of some boron containing resources for gamma ray and fast neutron. Results Phys. 2019;13:102-29.

14. Xiang C, Han EH, Zhang ZM, Fu HM, Wang JQ, Zhang HF, et al. Design of single-phase high-entropy alloys composed of low thermal neutron absorption cross-section elements for nuclear power plant application. Intermetallics. 2019;104:143-53.

15. Limkitjaroenporn P, Kaewkhao J, Chewpraditkul W, Limsuwan P. Mass Attenuation Coefficient and Effective Atomic Number of Ag/Cu/Zn Alloy at Different Photon Energy by Compton Scattering Technique. Procedia Engineer. 2012;32:847-54.

16. Khobkham C, Limkitjaroenporn P, Shimada K, Kaewkhao J, Chaiphaksa W. Photon interaction behavior of zirconium alloy materials. Materials Today: Proceedings. 2018;5:14928-32.

17. Kumar A. Gamma ray shielding properties of PbO-Li_2O-B_2O_3 glasses. Radiat Phys Chem. 2017;136:50-3.

18. Chanthima N, Kaewkhao J. Investigation on radiation shielding parameters of bismuth borosilicate glass from 1 keV to 100 GeV. Ann Nucl Energy. 2013;55:23-8.

19. Kaur K, Singh KJ, Anand V. Structural properties of Bi_2O_3-B_2O_3-SiO_2-Na_2O glasses for gamma ray shielding applications. Radiat Phys Chem. 2016;120:63-72.

20. El-bashir BO, Sayyed MI, Zaid MHM, Matori KA. Comprehensive study on physical, elastic

and shielding properties of ternary BaO-Bi_2O_3-P_2O_5 glasses as a potent radiation shielding material. J Non-Cryst Solids. 2017;468:92-9.

21. Dong MG, Sayyed MI, Lakshminarayana G, Çelikbilek Ersundu M, Ersundu AE, Nayar P, et al. Investigation of gamma radiation shielding properties of lithium zinc bismuth borate glasses using XCOM program and MCNP5 code. J Non-Cryst Solids. 2017;468:12-6.

22. Vishwanath PS, Badiger NM, Chanthima N, Kaewkhao J. Evaluation of gamma-ray exposure buildup factors and neutron shielding for bismuth borosilicate glasses. Radiat Phys Chem. 2014;98:14-21.

23. Oto B, Yıldız N, Korkut T, Kavaz E. Neutron shielding qualities and gamma ray buildup factors of concretes containing limonite ore. Nucl Eng Des. 2015;293:166-75.